Available online at www.sciencedirect.com
ScienceDirect
Trans. Nonferrous Met. Soc. China 31(2021) 832−841
Transactions of Nonferrous Metals Society of China
www.tnmsc.cn

Physicochemical properties of 1,3-dimethyl-2-imidazolinone−$ZnCl_2$ solvated ionic liquid and its application in zinc electrodeposition

Ai-min LIU[1], Meng-xia GUO[1], Zhong-ning SHI[2], Yu-bao LIU[3],
Feng-guo LIU[1], Xian-wei HU[1], You-jian YANG[1], Wen-ju TAO[1], Zhao-wen WANG[1]

1. Key Laboratory for Ecological Metallurgy of Multimetallic Mineral (Ministry of Education), Northeastern University, Shenyang 110819, China;
2. State Key Laboratory of Rolling and Automation, Northeastern University, Shenyang 110819, China;
3. State Key Laboratory of Baiyunobo Rare Earth Resource Researches and Comprehensive Utilization, Baotou Research Institute of Rare Earths, Baotou 014030, China

Received 12 April 2020; accepted 10 November 2020

Abstract: Zinc chloride ($ZnCl_2$) was dissolved in the 1,3-dimethyl-2-imidazolinone (DMI) solvent, and the metallic zinc coatings were obtained by electrodeposition in room-temperature ambient air. The conductivity (σ), viscosity (η), and density (ρ) of the DMI−$ZnCl_2$ solvated ionic liquid at various temperatures (T) were measured and fitted. Furthermore, cyclic voltammetry was used to study the electrochemical behavior of Zn(II) in the DMI−$ZnCl_2$ solvated ionic liquid, indicating that the reduction of Zn(II) on the tungsten electrode was a one-step two-electron transfer irreversible process. XRD and SEM−EDS analysis of the cathode product confirmed that the deposited coating was metallic zinc. Finally, the effects of deposition potential, temperature and duration on the morphology of zinc coatings were investigated. The results showed that a dense and uniform zinc coating was obtained by potentiostatic electrodeposition at −2 V (vs Pt) and 353 K for 1 h.

Key words: electrodeposition; zinc; 1,3-dimethyl-2-imidazolinone; physicochemical properties; cyclic voltammetry

1 Introduction

Zinc is usually deposited on the surface of steel materials to obtain a dense and uniform coating with excellent adhesion. Zinc, used as a sacrificial anode, can protect the steel materials against corrosion [1]. Conditional production of zinc coatings was carried out with electrodeposition in the aqueous cyanide, basic non-cyanide, and chloride solutions. However, the electrodeposition of zinc in aqueous solutions has disadvantages such as hydrogen embrittlement, wastewater treatment, and low current efficiency [2,3]. Thus, it is of significant direction to seek new solvents from which high-quality zinc coatings can be deposited without environmental pollution.

In recent years, the electrodeposition of zinc and its alloys in ionic liquids have attracted increasing attention from researchers. Compared with aqueous solutions, ionic liquids have better thermal stability, lower vapor pressure, and wider electrochemical windows [4−6]. LIN and SUN [7] reported that zinc could be electrodeposited from the $ZnCl_2$−1-methyl-3-ethylimidazolium chloride ($ZnCl_2$−MEIC with molar ratio of 1:1) and $ZnCl_2$−$AlCl_3$−MEIC ionic liquid at potential of −0.8 V (vs Al). HSIU et al [8] investigated the influence of electrolyte composition on the electrochemical window of the $ZnCl_2$−1-ethyl-3-methylimidazolium chloride ($ZnCl_2$−EMIC) ionic liquid, indicating that the electrochemical window

Corresponding author: Zhong-ning SHI; Tel: +86-24-83686381; E-mail: znshi@mail.neu.edu.cn
DOI: 10.1016/S1003-6326(21)65542-5

was −2 V when the $ZnCl_2$−EMIC ionic liquid was acidic, and zinc coating was able to deposit at −0.05 V (vs Zn) and 383 K. DENG et al [9] electrodeposited zinc in the N-butyl-N-methyl-pyrrolidinium dicyandiamide (BMP-DCA) ionic liquid containing $ZnCl_2$ at −2.4 V (vs Fc/Fc^+) and 323 K. Zn and Zn−Au alloy were obtained on a Au electrode by electrodeposition in the $ZnCl_2$−1-butyl-3-methylimidazolium chloride ($ZnCl_2$−BMIC with molar ratio of 3:2) ionic liquid, while Zn−Co alloy was produced from the $ZnCl_2$−BMIC ionic liquid containing 1.16 wt.% $CoCl_2$ [10,11]. However, above ionic liquids are expensive, and electrodeposition experiments should be performed in a glove box filled with inert gas because these ionic liquids are sensitive to the air and water, which greatly limits their industrial application.

Deep eutectic solvents (DES), which were first described by ABBOTT in 2003, have been widely studied for electrochemical application due to their low cost. XU et al [12] obtained Zn−Ti alloy by electrodeposition in the $ZnCl_2$−urea (molar ratio of 3:1) DES containing 0.27 mol/L $TiCl_4$ at 353 K. YANG et al [13] prepared Zn−Ni alloy coating from the choline chloride−urea (ChCl−urea with molar ratio of 1:2) DES containing 0.1 mol/L $NiCl_2$ and 0.4 mol/L $ZnCl_2$ at 343 K, while CHU et al [14] prepared Zn−Co alloy coating from the DES containing 0.11 mol/L $ZnCl_2$ and 0.01 mol/L $CoCl_2$. LI et al [15] added 0.10 g/L GO (graphene oxide) to the ChCl−urea DES containing 0.2 mol/L $ZnCl_2$, and successfully produced a novel Zn−GO composite coating by pulse electrodeposition. SANCHEZ et al [16] prepared Zn−Ce coating in the ChCl-urea DES containing 0.3 mol/L $ZnCl_2$ and 0.1 mol/L $CeCl_3$. LI et al [17] electrodeposited Zn−Ni alloy coatings with controllable components and excellent corrosion resistance by adding 5 wt.% water to the ChCl−urea DES containing 0.08 mol/L $NiCl_2$ and 0.4 mol/L $ZnCl_2$. BAO et al [18] explored the electrochemical deposition of Zn from lactate−ChCl (molar ratio of 2:1) at a constant current density of 10 mA/cm^2. BAKKAR and NEUBERT [19] obtained bulk Zn layers from the ChCl−urea−EG (ethylene glycol) DES (molar ratio of 1:1.5:0.5) at potential ranging from −1.2 to −1.5 V (vs Ag). VIEIRA et al [20] investigated the electrochemical behavior of zinc in the ChCl−EG (molar ratio of 1:2) DES containing $ZnCl_2$ on different electrodes including glassy carbon, stainless steel, Au, Pt, Cu and Zn. PEREIRA et al [21] prepared zinc from the ChCl−EG DES containing 5×10^{-4} mol/mL $ZnCl_2$, and found that the additive of dimethyl sulfoxide (DMSO) could achieve grain refinement and produce zinc with a minimum grain size of 31.7 nm. ALESARY et al [22] obtained a bright zinc coating by adding nicotinic acid, boric acid, and benzoquinone to the ChCl−EG DES containing 6×10^{-4} mol/mL $ZnCl_2$.

ENDO et al [23] found that a smooth aluminium film can be obtained by electrodeposition in the 1,3-dimethyl-2-imidazolidinone−$AlCl_3$ (DMI−$AlCl_3$) ionic liquid at 313 K when the content of $AlCl_3$ was higher than 50 at.%. Recently, ZHANG et al [24] reported an exceptional organic solvent composed of DMI and $LiNO_3$, and directly deposited a La film from $LaCl_3$ at −2.3 V (vs Ag) and 298 K. It was found that the DMI solvent has good solubility and coordination ability for chlorides, and it has advantages including low cost, low melting point, being insensitive to water, and wide electrochemical window. In this work, $ZnCl_2$ was dissolved in the DMI solvent for zinc electrodeposition. The conductivity, viscosity and density of the DMI−$ZnCl_2$ solvated ionic liquid at different temperatures were measured. Furthermore, the solubilities of $ZnCl_2$ in the DMI solvent at different temperatures were measured, and the electrochemical behavior of Zn(II) in DMI−$ZnCl_2$ ionic liquid was investigated by cyclic voltammetry and potentiostatic electrodeposition.

2 Experimental

Zinc chloride ($ZnCl_2$, 98%) and 1,3-dimethyl-2-imidazolidinone (DMI, 99%) were purchased from Shanghai Aladdin Bio-Chem Technology Co., Ltd., China. The DMI−$ZnCl_2$ solvated ionic liquid was prepared by adding 0.29 g/mL $ZnCl_2$ to the DMI solvent and stirring on a magnetic heating plate in ambient atmosphere. The conductivity, viscosity, and density of the ionic liquid were measured based on the fixed cell constant method, the rotation method, and the Archimede's principle, respectively. Moreover, the solubilities of $ZnCl_2$ in the DMI solvent were measured by the equilibrium method.

Cyclic voltammetry was performed using a three-electrode system by a electrochemical workstation (CHI600E, Shanghai Chenhua

Instrument, Shanghai, China). A tungsten wire (99.99%, diameter of 1 mm) was used as the working electrode, while two platinum wires (99.99%, diameter of 1 mm) were used as the counter electrode and the reference electrode, respectively. The surface of electrodes were polished with sandpapers, cleaned with ethanol and deionized water, and then dried before the measurement of cyclic voltammogram. The working electrode was immersed in the ionic liquid with depth of 1.4 cm.

Electrodeposition experiments were also carried out using a three-electrode system by the CHI600E electrochemical workstation. The working electrode was a tungsten sheet (99.99%, side area of 1 cm^2), while the counter electrode and the reference electrode were platinum wires. After electrodeposition experiments, the surface of the working electrode was washed with acetone and distilled water, dried naturally and then stored in a glove box, in which the contents of water and oxygen were below 1×10^{-6}. X-ray diffraction (XRD, D8 ADVANCE, Bruker, Germany) was used to analyze the phase structure of the zinc deposited on tungsten substrates. In addition, the surface morphology and elemental composition of zinc coatings were studied by a scanning electron microscope (SEM, ULTRA PLUS, Zeiss Microscope, Germany) combined with X-ray dispersive energy spectrometer (EDS).

3 Results and discussion

3.1 Physical and chemical properties of DMI−$ZnCl_2$ solvated ionic liquid

The relationship between the conductivities of the DMI−$ZnCl_2$ solvated ionic liquid and temperature (313−303 K) is shown in Fig. 1(a). It can be seen that the conductivity increased from 0.571 to 0.932 mS/cm when the temperature increased from 313 to 363 K. This was because the increase of the temperature was beneficial to the diffusion of ions in the ionic liquid, which promoted the mass transfer rate and caused the increased of conductivity. However, the increase rate of conductivity was small at 353−363 K.

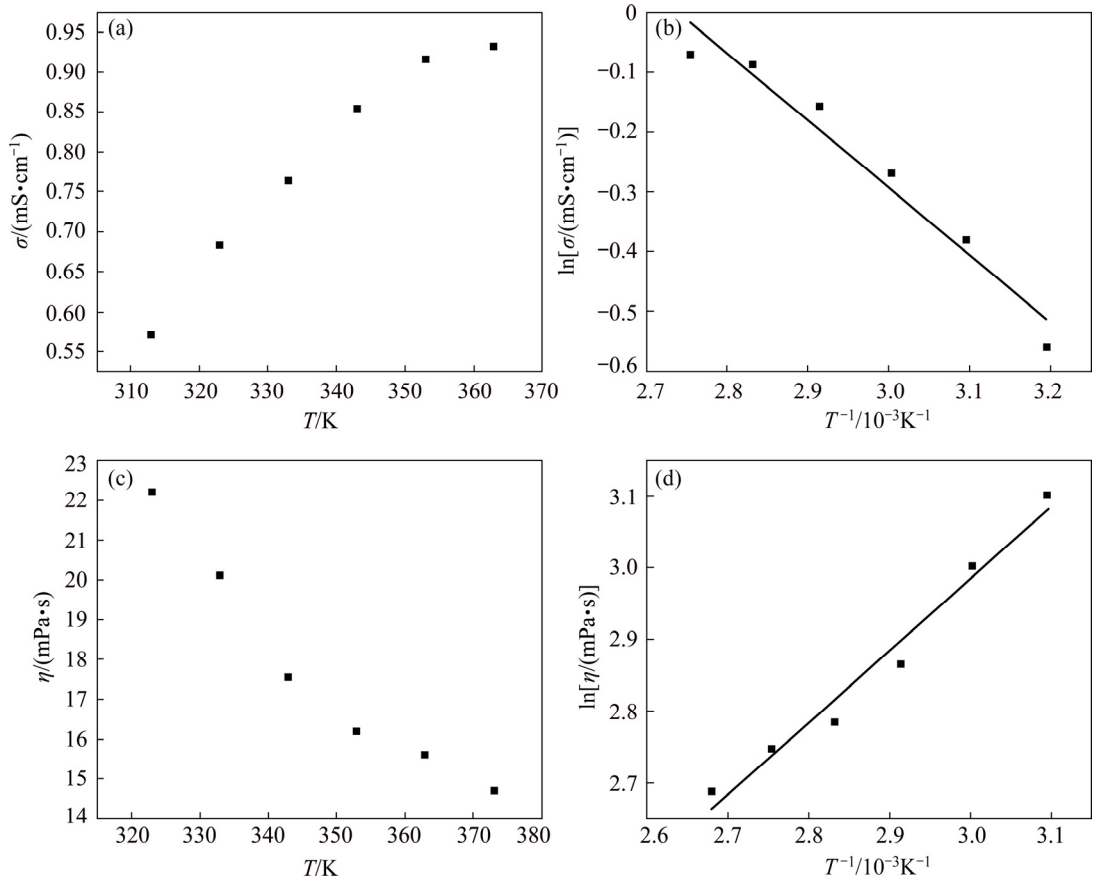

Fig. 1 Conductivities of DMI−$ZnCl_2$ solvated ionic liquid as function of temperature (a), relationship between ln σ and T^{-1} (b), viscosities of DMI−$ZnCl_2$ solvated ionic liquid as function of temperature (c) and relationship between ln η and T^{-1} (d)

The conductivity of the DMI−$ZnCl_2$ solvated ionic liquid was of the same order of magnitude as that of some conventional ionic liquids ranging from 0.1 to 10 mS/cm [25]. For example, the conductivity of the EMIC ionic liquid at 298 K was reported to be 3.43−3.71 mS/cm [26]. In comparison, the conductivity of the DMI−$ZnCl_2$ solvated ionic liquid was much smaller than that of the aqueous solution containing 3.7 mol/L $ZnCl_2$ at 298 K (107 mS/cm) [27]. However, the conductivity of the DMI−$ZnCl_2$ solvated ionic liquid was larger than that of the urea−$ZnCl_2$ (molar ratio of 3:1) DES at 298 K (0.051 mS/cm) [12], and the urea−$ZnCl_2$ (molar ratio of 3.5:1) and ChCl−$ZnCl_2$ (molar ratio of 1:2) DES at 315 K (0.18 and 0.06 mS/cm, respectively) [28]. As we know, the DMI solvent is an organic liquid with small conductivity. Therefore, it can be indicated that the conductivity of the DMI solvent was modified by the Lewis acidic cation Zn(II), and the DMI−$ZnCl_2$ solvated ionic liquid that has similar characteristics as conventional ionic liquid was obtained.

In general, the relationship between the conductivity of ionic liquid and temperature can be expressed using the Arrehnius equation [25]:

$$\ln \sigma=\ln \sigma_0-E_\sigma/(RT) \quad (1)$$

where σ is the conductivity (mS/cm), σ_0 is a pre-factor (mS/cm), E_σ is the conductivity activation energy (kJ/mol), R is the ideal gas constant (8.314 $J\cdot K^{-1}\cdot mol^{-1}$), and T is the temperature (K). As shown in Fig. 1(b), there was a good linear relationship between $\ln \sigma$ and T^{-1}. Through linear fitting, the relationship between the conductivity of DMI−$ZnCl_2$ solvated ionic liquid and temperature can be expressed by Eq. (2), and the activation energy of the conductivity was determined to be 9.387 kJ/mol:

$$\ln \sigma=3.095-1129.059/T \quad (2)$$

The high viscosity of ionic liquids is one of the bottlenecks preventing them from gaining large-scale industrial applications. In general, the viscosity of ionic liquid is determined by the internal van der WAALS force and the interaction of hydrogen bonds. Thus, suitable additives are added to the ionic liquid to reduce the viscosity. In this work, the viscosities of the DMI−$ZnCl_2$ solvated ionic liquid at 323−373 K were measured by the rotation method. The relationship between the viscosities of the DMI−$ZnCl_2$ solvated ionic liquid and temperature is shown in Fig. 1(c). The viscosity decreased with increasing temperature because the van der WAALS force and hydrogen bond strength within the system changed with temperature. Furthermore, the relationship between viscosity and temperature can be expressed by the Arrhenius formula [29]:

$$\ln \eta=\ln \eta_0+E_\eta/(RT) \quad (3)$$

where η is viscosity (mPa·s), η_0 is a pre-factor (mPa·s), and E_η is the activation energy of viscosity (kJ/mol). As shown in Fig. 1(d), there was a good linear relationship between $\ln \eta$ and T^{-1}. By linear fitting, the relationship between the viscosity of DMI−$ZnCl_2$ solvated ionic liquid and temperature can be expressed by Eq. (4), and the activation energy of the viscosity was determined to be 8.364 kJ/mol:

$$\ln \eta=-0.033+1006.014/T \quad (4)$$

The densities of the DMI−$ZnCl_2$ solvated ionic liquid at 313−373 K were measured by the Archimede's principle. The relationship between the densities of the DMI−$ZnCl_2$ solvated ionic liquid and temperature is shown in Fig. 2.

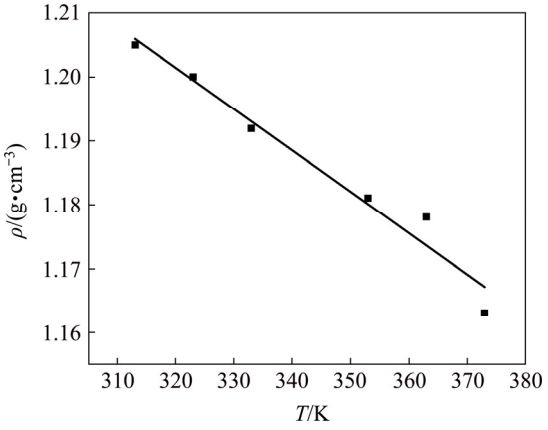

Fig. 2 Densities of DMI−$ZnCl_2$ solvated ionic liquid as function of temperature

It can be found from Fig. 2 that the density demonstrated a linear relationship with temperature. Besides, the density gradually decreased from 1.205 to 1.163 g/cm^3 with temperature increasing from 313 to 373 K, and the trend was relatively flat. This is because when the temperature increased, the migration rate and spacing of particles in the ionic liquid increased, which caused the expansion of volume. Since the number of particles per unit area was diminished at higher temperature, the density became smaller. Through linear fitting, the densities

of the DMI−$ZnCl_2$ solvated ionic liquid at different temperatures can be expressed using the following equation:

$$\rho=-6.464\times10^{-4}T+1.406 \quad (5)$$

where ρ is the density (g/cm^3).

The concentration of $ZnCl_2$ in the DMI−$ZnCl_2$ solvated ionic liquid is an important parameter during the process of zinc electrodeposition. Hence, the effect of temperature on the solubilities of $ZnCl_2$ in the DMI solvent was explored. The solubilities of $ZnCl_2$ in the DMI solvent at 313, 333, 353 and 373 K were determined to be 0.29, 0.32, 0.45, and 1.58 g/mL, respectively. With temperature increasing from 313 to 353 K, the solubility of $ZnCl_2$ gradually increased from 0.29 to 0.45 g/mL. It was worth noting that when the temperature increased from 353 to 373 K, the solubilities of $ZnCl_2$ significantly increased from 0.45 to 1.58 g/mL. However, the ionic liquid at 373 K became very viscous, and eventually turned into a transparent colloid which was no longer suitable for zinc electrodeposition. Therefore, it was not recommended to perform zinc electrodeposition experiments with saturated $ZnCl_2$ concentration, especially at temperature higher than 373 K. Therefore, the measurement of physicochemical properties and electrochemical experiments in this work were carried out in the DMI−$ZnCl_2$ solvated ionic liquid containing 0.29 g/mL $ZnCl_2$ at 313−373 K.

3.2 Electrochemical behavior of Zn(II) in DMI−$ZnCl_2$ solvated ionic liquid

The electrochemical behavior of Zn(II) ions in the DMI−$ZnCl_2$ solvated ionic liquid at 313 K was studied by cyclic voltammetry using a tungsten working electrode. It can be seen from Fig. 3(a) that the cyclic voltammetry curve from 1 to −3 V (vs Pt) was a straight line, and the current was almost zero, indicating that the DMI solvent was stable within this potential range. When 0.29 g/mL $ZnCl_2$ was dissolved in the DMI solvent, a pair of redox peaks were found within the electrochemical window of the DMI solvent. Obviously, the reduction peak corresponds to the reduction of Zn(II) ions to metallic zinc, while the oxidation peak was related to the peeling of metal zinc from the electrode surface. The onset potential of the reduction of Zn(II) ions was −1.13 V (vs Pt), and the potential of the oxidation peak was −0.13 V (vs Pt).

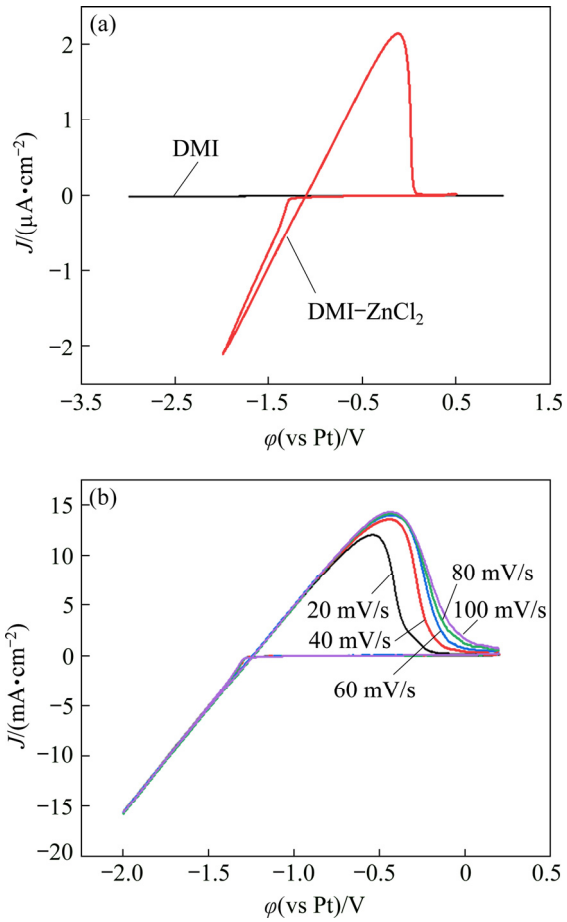

Fig. 3 Cyclic voltammetry curves on tungsten electrode in DMI solvent and DMI−$ZnCl_2$ solvated ionic liquid at 313 K (scan rate of 40 mV/s) (a) and in DMI−$ZnCl_2$ solvated ionic liquid at 353 K and different scan rates (b)

As seen in Fig. 3(b), the current densities of the oxidation peaks increased as the scan rate increased from 20 to 100 mV/s, and the potential of the oxidation peaks shifted to the more positive values. However, the scan rate had no obvious influence on the current density and potential of the reduction peak, indicating that the reduction reaction was not controlled by diffusion. Besides, only one reduction signal was observed. Therefore, the reduction of Zn(II) was a one-step two-electron transfer irreversible reaction process. Moreover, it should be noted that a “nucleation loop” related to the nucleation of the deposited zinc was observed.

3.3 Effect of deposition potential, temperature and duration on zinc coatings

The process of metal electrodeposition includes the formation and growth of crystal nuclei, and overpotential is the driving force for nucleation. According to the analysis from the cyclic

voltammetry curve, different potentials were applied to the electrodeposition experiments performed at 353 K for 1 h. The XRD patterns of the cathode products obtained by deposition at potentials of −1.4, −1.6, −1.8 and −2 V (vs Pt) are shown in Fig. 4(a). The characteristic peaks at 2θ=57.9° and 72.8° were corresponding to the tungsten substrate, while the other diffraction peaks in the XRD patterns matched well with the characteristic peaks of zinc (ICDD 00-004-0836), which confirmed that the cathode product was metallic zinc [30]. As the applied potential shifted from −1.4 V to more negative potential of −2 V, the intensity of the XRD diffraction peak for zinc became greater, indicating that the zinc coating deposited on the surface of tungsten substrate at −2 V was thicker. Moreover, the preferred orientations for zinc crystal growth were the (002) and (101) planes.

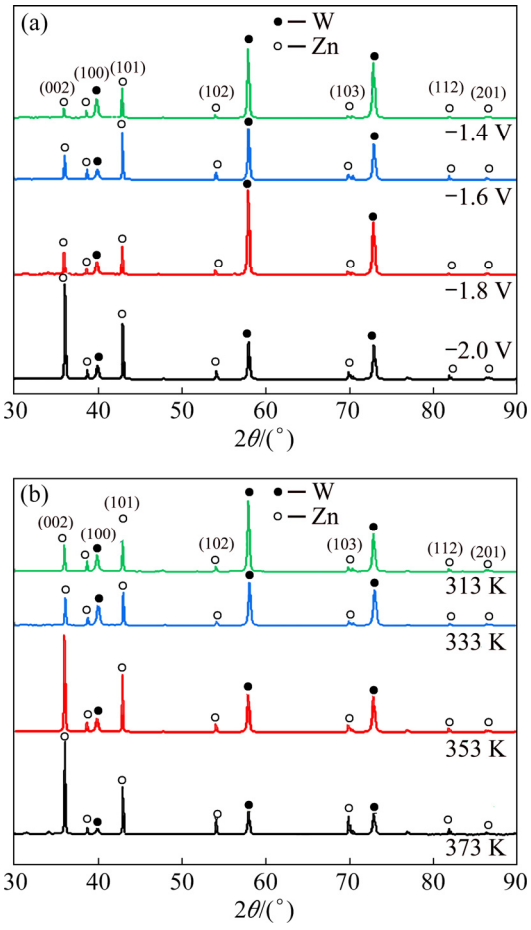

Fig. 4 XRD patterns of zinc coatings obtained by electrodeposition on tungsten electrode in DMI−$ZnCl_2$ solvated ionic liquid for 1 h: (a) At 353 K and different potentials (from −1.4 to −2 V (vs Pt)); (b) At −2 V (vs Pt) and different temperatures (from 313 to 373 K)

The effect of temperature on the zinc coating was studied by electrodeposition experiments performed at −2 V (vs Pt) for 1 h. The XRD patterns of the cathode products obtained by electrodeposition at temperatures of 313, 333, 353 and 373 K are shown in Fig. 4(b). When the temperature increased from 313 to 353 K, the intensity of the XRD diffraction peak for zinc increased. However, when the electrodeposition temperature increased from 353 to 373 K, the intensity of the XRD diffraction peak for zinc did not continue to increase. Based on the analysis from XRD patterns, it could be concluded that a better zinc coating was obtained by electrodeposition at −2 V (vs Pt) and 353 K.

As shown in the inset of Fig. 5(a), a dark gray coating was obtained on the surface of the tungsten substrate by electrodepositing in the DMI−$ZnCl_2$ solvated ionic liquid at −2 V (vs Pt) and 353 K. The SEM image (Fig. 5(a)) showed that the coating obtained by potentiostatic electrodeposition at −2 V (vs Pt) and 353 K was dense and uniform, which

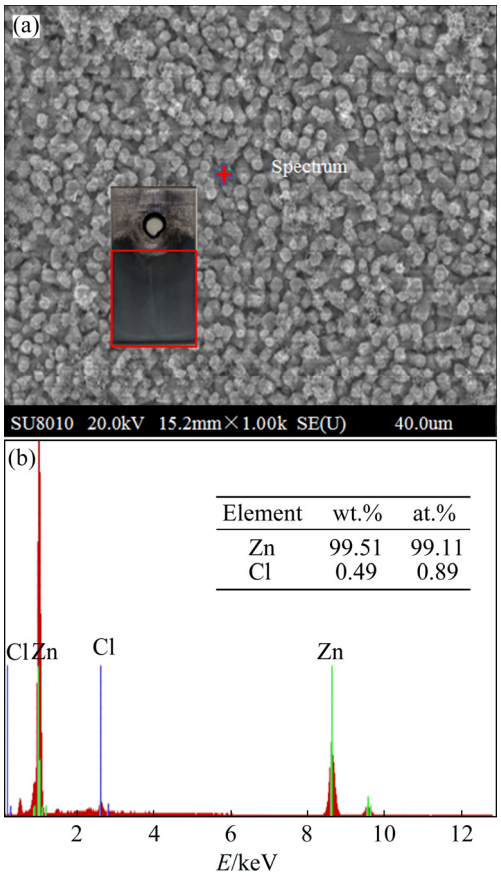

Fig. 5 SEM image (a) and EDS spectrum (b) of zinc coating obtained by electrodeposition on tungsten electrode in DMI−$ZnCl_2$ solvated ionic liquid at −2 V (vs Pt) and 353 K for 1 h

was in accordance with the results from XRD analysis. In addition, the EDS spectrum of the coating demonstrated that the elemental compositions of the coating were 99.51 wt.% Zn and 0.49 wt.% Cl. The small amount of Cl element came from the ionic liquid containing $ZnCl_2$.

The SEM images of the cathode coatings obtained by potentiostatic electrodeposition at different potentials (vs Pt) and temperatures are shown in Figs. 6 and 7, respectively. From Fig. 6,

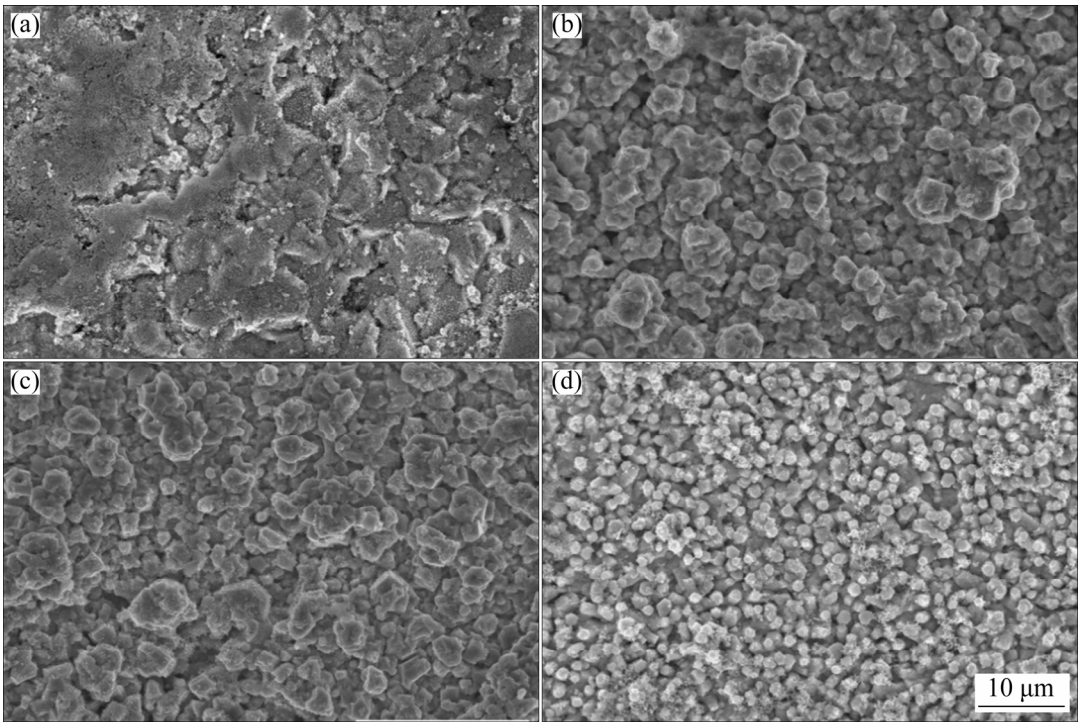

Fig. 6 SEM images of zinc coatings obtained by electrodeposition on tungsten electrodes in DMI−$ZnCl_2$ solvated ionic liquid at 353 K and various potentials (vs Pt) for 1 h: (a) −1.4 V; (b) −1.6 V; (c) −1.8 V; (d) −2 V

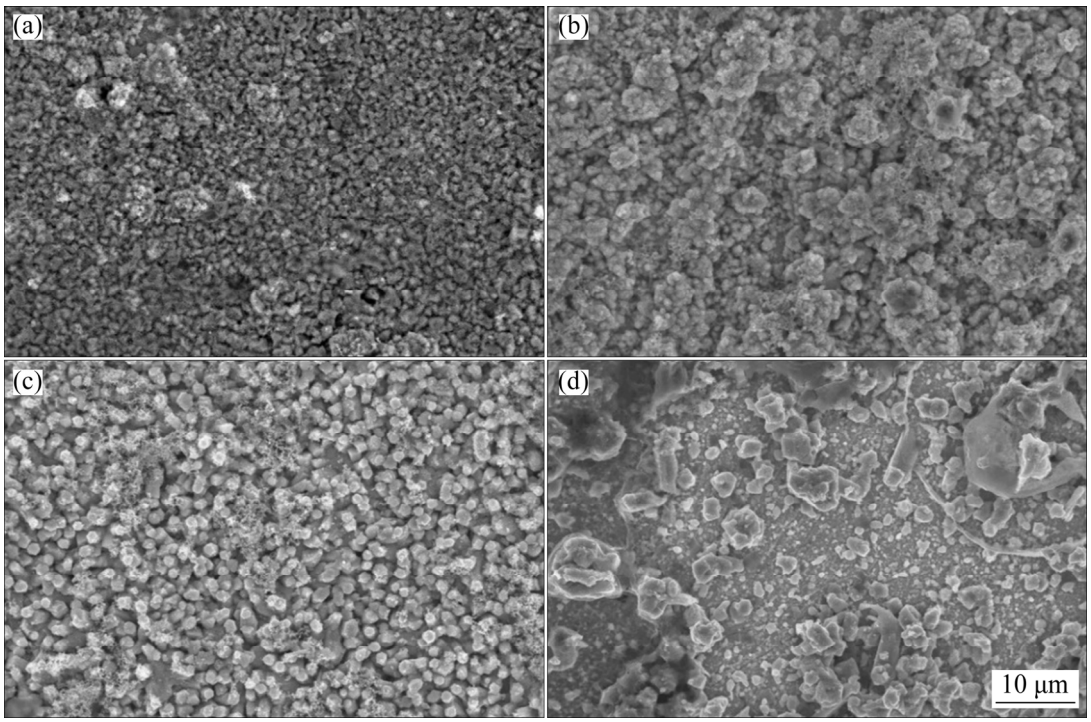

Fig. 7 SEM images of zinc coatings obtained by electrodeposition on tungsten electrodes in DMI−$ZnCl_2$ solvated ionic liquid at −2 V (vs Pt) and different temperatures for 1 h: (a) 313 K; (b) 333 K; (c) 353 K; (d) 373 K

when the potential changed from −1.4 to −2 V (vs Pt), the grain size of the deposited metal zinc became smaller because the nucleation density and nucleation rate increased as the applied potential shifted to the more negative values. Moreover, the crystal morphology changed from irregular to hexagonal particles, and a uniform zinc coating was obtained by electrodeposition at −2 V (vs Pt). LIN and SUN [7] proposed similar results about the influence of potential on the micro-morphology of zinc coating deposited from the $AlCl_3$−MEIC−$ZnCl_2$ ionic liquid.

From Fig. 7, as the temperature increased from 313 to 373 K, the grain size of the deposited metal zinc became larger. It could be explained that with the increase of temperature, the driving force of ion migration and the growth of metal core were accelerated, which resulted in the increase of grain size. XU et al [12] reported similar results about the influence of temperature on the micro-morphology of Zn−Ti alloy prepared by electrodeposition in the urea−$ZnCl_2$ deep eutectic solvent.

Figure 8(a) exhibits the XRD patterns of zinc coatings obtained by electrodeposition on tungsten electrodes at −2 V (vs Pt) and 353 K for different durations. The characteristic peaks of metallic zinc were observed on all of the XRD patterns. When the deposition time was 0.5 h, the characteristic peaks of the tungsten substrate were obvious. As the deposition time was extended, the intensity of the zinc characteristic peaks increased due to the changes of the thickness of zinc coatings, which was further confirmed by the cross-sectional SEM images as demonstrated in Fig. 8(b). When the deposition time increased from 0.5 to 2 h, the thickness of zinc coatings increased approximately from 6.7 to 32 μm.

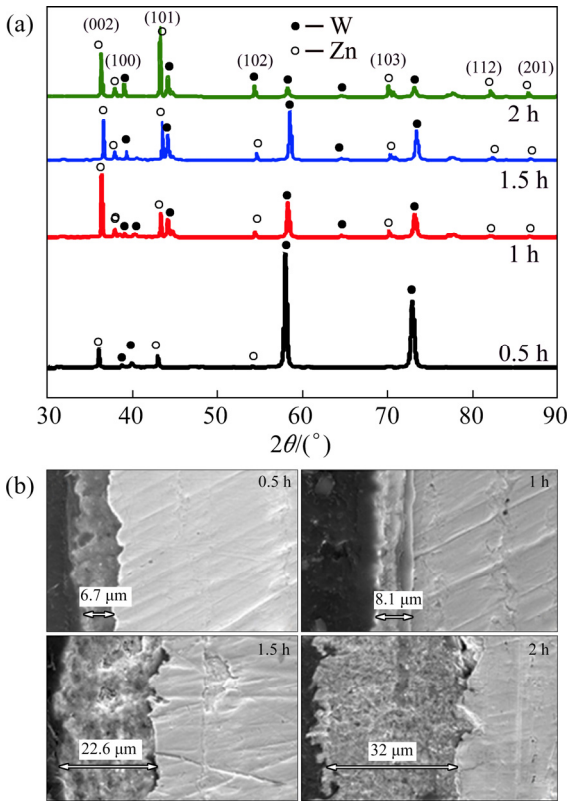

Fig. 8 XRD patterns (a) and SEM images (b) for cross section of zinc coatings obtained by electrodeposition on tungsten electrodes in DMI−$ZnCl_2$ solvated ionic liquid at −2 V (vs Pt) and 353 K for different durations

4 Conclusions

(1) The conductivities of the DMI−$ZnCl_2$ solvated ionic liquid at 313−363 K were in the range of 0.571−0.932 mS/cm, which can be expressed by $\ln \sigma=3.095-1129.059/T$.

(2) The viscosities and densities of the DMI−$ZnCl_2$ solvated ionic liquid were in the range of 22.20−14.70 mPa·s (323−373 K) and 1.205−1.163 g/cm^3 (313−373 K), which can be expressed by $\ln \eta=-0.033+1006.014/T$ and $\rho=-6.464\times10^{-4}T+1.406$, respectively.

(3) The solubilities of $ZnCl_2$ in the DMI solvent at 313 K was 0.29 g/mL, and $ZnCl_2$ was used as precursor to electrodeposite zinc coatings in the DMI−$ZnCl_2$ solvated ionic liquid at room temperature and ambient air.

(4) Results from cyclic voltammetry showed that the onset reduction potential of zinc was −1.13 V (vs Pt). XRD and SEM−EDS analysis confirmed that metallic zinc was obtained by electrodeposition for 1 h, while the preferred deposition potential and temperature were −2 V (vs Pt) and 353 K.

Acknowledgments

The authors are grateful for the financial supports from the Fundamental Research Funds for the Central Universities, China (N182503033, N172502003), Postdoctoral Research Foundation of China (2018M640258), the National Natural Science Foundation of China (51804070) and Guangxi Innovation-driven Development Program, China (GUIKE AA18118030).

References

[1] KRISHNAN R M, NATARAJAN S R, MURALIDHARAN V S, SINGH G. Characteristics of a non-cyanide alkaline zinc plating bath [J]. Plating and Surface Finishing, 1992, 79: 67−70.

[2] RAMESH BAPU G N K, DEVARAJ G, AYYAPPARAJ J. Studies on non-cyanide alkaline zinc electrolytes [J]. Journal of Solid State Electrochemistry, 1998, 3: 48−51.

[3] LIU Z, ZEIN El ABEDIN S, ENDRES F. Electrodeposition of zinc films from ionic liquids and ionic liquid/water mixtures [J]. Electrochimica Acta, 2013, 89: 635−643.

[4] WELTON T. Room-temperature ionic liquids: Solvents for synthesis and catalysis [J]. Chemical Reviews, 1999, 99: 2071−2083.

[5] ENDRES F. Ionic liquids: Solvents for the electrodeposition of metals and semiconductors [J]. Chem Phys Chem, 2002, 3: 144−154.

[6] HUANG Jing-fang, SUN I W. Nonanomalous electrodeposition of zinc−iron alloys in an acidic zinc chloride-1-ethyl-3-methylimidazolium chloride ionic liquid [J]. Journal of The Electrochemical Society, 2004, 151: C8−C14.

[7] LIN Yu-feng, SUN I W. Electrodeposition of zinc from a mixture of zinc chloride and neutral aluminum chloride-1-methyl-3-ethylimidazolium chloride molten salt [J]. Journal of The Electrochemical Society, 1999, 146: 1054−1059.

[8] HSIU S I, HUANG Jing-fang, SUN I W, YUAN Cheng-hui, SHIEA J. Lewis acidity dependency of the electrochemical window of zinc chloride-1-ethyl-3-methyl imidazolium chloride ionic liquids [J]. Electrochimica Acta, 2002, 47: 4367−4372.

[9] DENG M J, LIN P C, CHANG J K, CHEN Jin-ming, LU K T. Electrochemistry of Zn(II)/Zn on Mg alloy from the N-butyl-N-methylpyrrolidinium dicyanamide ionic liquid [J]. Electrochimica Acta, 2011, 56: 6071−6077.

[10] BORISSOV D, PAEEEK A, RENNER F U, ROHWERDER M. Electrodeposition of Zn and Au−Zn alloys at low temperature in an ionic liquid [J]. Physical Chemistry Chemical Physics, 2010, 12: 2059−2062.

[11] CHEN Po-yu, SUN I W. Electrodeposition of cobalt and zinc cobalt alloys from a Lewis acidic zinc chloride-1-ethyl-3-methylimidazolium chloride molten salt [J]. Electrochimica Acta, 2001, 46: 1169−1177.

[12] XU Cun-ying, WU Qing, HUA Yi-xin, LI Jian. The electrodeposition of Zn−Ti alloys from $ZnCl_2$−urea deep eutectic solvent [J]. Journal of Solid State Electrochemistry, 2014, 18: 2149−2155.

[13] YANG H Y, GUO X W, CHEN X B, WANG S H, WU G H, DING W J, BIRBILIS N. On the electrodeposition of nickel–zinc alloys from a eutectic-based ionic liquid [J]. Electrochimica Acta, 2012, 63: 131−138.

[14] CHU Qing-wei, LIANG Jun, HAO Jing-cheng. Electrodeposition of zinc−cobalt alloys from choline chloride–urea ionic liquid [J]. Electrochimica Acta, 2014, 115: 499−503.

[15] LI Rui-qian, LIANG Jun, HOU Yuan-yuan, CHU Qing-wei. Enhanced corrosion performance of Zn coating by incorporating graphene oxide electrodeposited from deep eutectic solvent [J]. The Royal Society of Chemistry Advances, 2015, 5: 60698−60707.

[16] SANCHEZ M M, ESCOSA E G, CONDE A, PALACIO C, GARCIA I. Deposition of zinc–cerium coatings from deep eutectic ionic liquids [J]. Materials, 2018, 11: 2035−2053.

[17] LI Rui-qian, DONG Qiu-jing, XIA Juan, LUO Chun-hua, SHENG Liang-quan, CHENG Feng, LIANG Jun. Electrodeposition of composition controllable Zn−Ni coating from water modified deep eutectic solvent [J]. Surface & Coatings Technology, 2019, 366: 138−145.

[18] BAO Quan-he, ZHAO Li-qing, JING He-ming, MAO Ang. Electrodeposition of zinc from low transition temperature mixture formed by choline chloride+lactic acid [J]. Materials Today, 2018, 14: 249−253.

[19] BAKKAR A, NEUBERT V. Recycling of cupola furnace dust: Extraction and electrodeposition of zinc in deep eutectic solvents [J]. Journal of Alloys and Compounds, 2019, 771: 424−432.

[20] VIEIRA L, SCHENNACH R, GOLLAS B. The effect of the electrode material on the electrodeposition of zinc from deep eutectic solvents [J]. Electrochimica Acta, 2016, 197: 344−352.

[21] PEREIRA N M, PEREIRA C M, ARAUJO J P, SILVA A F. Zinc electrodeposition from deep eutectic solvent containing organic additives [J]. Journal of Electroanalytical Chemistry, 2017, 801: 545−551.

[22] ALESARY H F, CIHANGIR S, BALLANTYNE A D, HARRIS R C, WESTON D P, ABBOTT A P, RYDER K S. Influence of additives on the electrodeposition of zinc from a deep eutectic solvent [J]. Electrochimica Acta, 2019, 304: 118−130.

[23] ENDO A, MIYAKE M, HIRATO T. Electrodeposition of aluminum from1,3-dimethyl-2-imidazolidinone/$AlCl_3$ baths [J]. Electrochimica Acta, 2014, 137: 470−475.

[24] ZHANG Bao-guo, YAO Yu, SHI Zhong-ning, XU Jun-li, LIU Yu-bao, WANG Zhao-wen. Communication—Direct room-temperature electrodeposition of La from $LaCl_3$ in an organic solvent supported by $LiNO_3$ [J]. Journal of the Electrochemical Society, 2019, 166: D218−D220.

[25] KOEL M. Ionic liquids in chemical analysis [J]. Critical Reviews in Analytical Chemistry, 2005, 35: 177−192.

[26] ZHANG Suo-jiang, SUN Ning, HE Xue-zhong, LU Xing-mei, ZHANG Xian-ping. Physical properties of ionic liquids: Database and evaluation [J]. Journal of Physical and Chemical Reference Data, 2006, 35: 1475−1517.

[27] THOMAS B K, FRAY D J. The conductivity of aqueous zinc chloride solutions [J]. Journal of Applied Electrochemistry, 1982, 12: 1−5.

[28] HAMAD A A, HAYYAN M, AISAADI M A, HASHIM M A. Potential applications of deep eutectic solvents in nanotechnology [J]. Chemical Engineering Journal, 2015, 273: 551−567.

[29] YOSHIZAWA M, XU Wu, ANGELL C A. Ionic liquids by proton transfer: Vapor pressure, conductivity, and the relevance of ΔpK_a from aqueous solutions [J]. Journal of the American Chemical Society, 2003, 125: 15411−15419.

[30] YANG Hao-xing, REDDY R G. Electrochemical kinetics of reduction of zinc oxide to zinc using 2:1 urea/ChCl ionic liquid [J]. Electrochimica Acta, 2015, 178: 617−623.

1,3-二甲基-2-咪唑啉酮−$ZnCl_2$溶剂化离子液体的物化性质及在锌电沉积中的应用

刘爱民[1]，郭梦霞[1]，石忠宁[2]，刘玉宝[3]，刘风国[1]，胡宪伟[1]，杨酉坚[1]，陶文举[1]，王兆文[1]

1. 东北大学 多金属共生矿生态化冶金教育部重点实验室，沈阳 110819；
2. 东北大学 轧制技术及连轧自动化国家重点实验室，沈阳 110819；
3. 包头稀土研究院 白云鄂博稀土资源研究与综合利用国家重点实验室，包头 014030

摘　要：将 $ZnCl_2$ 溶解于 1,3-二甲基-2-咪唑啉酮(DMI)中，并在室温大气环境中电沉积得到金属锌涂层。测量不同温度下 DMI−$ZnCl_2$ 溶剂化离子液体的电导率(σ)、黏度(η)和密度(ρ)并拟合出方程式。然后，利用循环伏安法研究 Zn(II)在 DMI−$ZnCl_2$ 溶剂化离子液体中的电化学还原行为，发现 Zn(II)在钨电极上的还原为一步两电子的不可逆过程。阴极产物的 XRD 和 SEM−EDS 分析表明，沉积产物为金属锌。最后，考察沉积电位、温度和时间对锌镀层形貌的影响，结果表明，在−2 V (vs Pt)和 353 K 条件下恒电位电沉积 1 h，可得到致密均匀的锌涂层。

关键词：电沉积；锌；1,3-二甲基-2-咪唑啉酮；物理化学性质；循环伏安法

(Edited by Bing YANG)